

# RSC Advances



This is an *Accepted Manuscript*, which has been through the Royal Society of Chemistry peer review process and has been accepted for publication.

*Accepted Manuscripts* are published online shortly after acceptance, before technical editing, formatting and proof reading. Using this free service, authors can make their results available to the community, in citable form, before we publish the edited article. This *Accepted Manuscript* will be replaced by the edited, formatted and paginated article as soon as this is available.

You can find more information about *Accepted Manuscripts* in the [Information for Authors](#).

Please note that technical editing may introduce minor changes to the text and/or graphics, which may alter content. The journal's standard [Terms & Conditions](#) and the [Ethical guidelines](#) still apply. In no event shall the Royal Society of Chemistry be held responsible for any errors or omissions in this *Accepted Manuscript* or any consequences arising from the use of any information it contains.

## Synthesis and evaluation of macroporous polymerized solid acid derived from Pickering HIPEs for catalyzing cellulose into 5-hydroxymethylfurfural in ionic liquid

Heping Gao<sup>a</sup>, Yinxian Peng<sup>a\*</sup>, Jianming Pan<sup>b\*</sup>, Jun Zeng<sup>a</sup>, Changhua Song<sup>b</sup>, Yunlei Zhang<sup>b</sup>, Yongsheng Yan<sup>b</sup>, Weidong Shi<sup>b</sup>

<sup>a</sup> School of biology and Chemical Engineering, and Jiangsu University of science and technology , Zhenjiang 212013, China

<sup>b</sup> School of Chemistry and Chemical Engineering, and Jiangsu University, Zhenjiang 212013, China

### Abstract

Stable water-in-oil (W/O) Pickering high internal phase emulsions (HIPEs) with an internal phase volume fraction of 84.8% were firstly stabilized by both the hydrophobic silica nanoparticles and span 80. Then based on the obtained Pickering HIPEs, several macroporous polymerized solid acid (PDVB-SS-X-SO<sub>3</sub>H, X = 0, 0.2, 0.6) were prepared by polymerizing divinyl benzene (DVB) and sodium p-styrenesulfonate (SS), subsequently combined with sulfonating in H<sub>2</sub>SO<sub>4</sub>. As-prepared PDVB-SS-X-SO<sub>3</sub>H all possessed open-cell structure, interconnecting pores and strong acidity, and were adopted as catalysts to convert cellulose into 5-hydroxymethylfurfural (HMF) in the presence of [Emim]Cl-mediated solvents. The results showed that a maximum yield of 29.6% for PDVB-SS-0.2-SO<sub>3</sub>H, 12.9% for PDVB-SS-0-SO<sub>3</sub>H and 15.5% for PDVB-SS-0.6-SO<sub>3</sub>H under the same condition within 2.0 h at 120 °C, suggesting the pore sizes and strong acidic sites played a key role in cellulose conversion. PDVB-SS-X-SO<sub>3</sub>H can be very easily recycled at least four times without significant loss of activity. This research opened up a new method to synthesize the porous solid acid catalyst materials through Pickering HIPEs templates.

**Keywords:** Solid acid; Pickering HIPEs; Porous material; Cellulose; HMF

### 1. Introduction

With the decreasing of fossil fuel reserves, cellulose, an abundant and renewable resource, is paid close attention to replacing fossil fuel.<sup>1</sup> For using cellulose to produce fuel, producing 5-hydroxymethylfurfural (HMF) from cellulose by one step is a very important process.<sup>2</sup> In the literature, HMF can be simply converted into furan bio-fuels, which can replace fossil fuels and chemical by condensation and hydrogenolysis reactions. For example, HMF can be hydrogenolysed into 2, 5-dimethylfuran (2,5-DMF) which is a kind of potential development of fuel<sup>3</sup> with having higher energy density than ethanol, and 2,5-bis(hydromethyl)furan (2,5-BHF) and 2,5-diformylfuran (2,5-DFF) that are widely used in the synthesis of polymers can also be produced from HMF.<sup>4</sup> In recent years, the catalytic progress of cellulose into HMF has been investigated by various acid catalysts. Homogeneous acid catalysts such as HCl,<sup>5</sup> and organic acids,<sup>6</sup> were applied and high HMF yield were obtained from the degradation of cellulose. However, the disadvantages of difficult separation of the catalyst from the liquid reaction medium, environmental unfriendly, strong corrosion, and easy to corrosion of equipment limited the further application of in industry. With the enhancement of environmental protection awareness, the increasing heterogeneous acid catalysts are used frequently in the degradation of cellulose to HMF, due to environmentally friendly, better recyclability, green chemical processes, easy to separate the catalyst from the solution system, and reductive corrosion to equipment. What's more, in recent years, solid acid catalysts such as solid immobilized liquid acid, zeolites,<sup>7</sup> sulfide,<sup>8</sup> natural

clay minerals,<sup>9</sup> ion-exchanged resins,<sup>10</sup> heteropoly acids (HPA),<sup>11</sup> oxides,<sup>12</sup> metal salts,<sup>13</sup> sulfonated carbon-based solid acid<sup>14</sup> and polymer-based solid acid<sup>15</sup> are widely used in various acid-catalyzed reactions.

Recently, more and more researchers found that porous solid acid have extra-ordinary catalytic activities due to excellent thermal stability, adjustable pore, high specific surface area, lower density, high catalytic activity and environmentally friendly. For example, Fujian Liu et al.<sup>16</sup> successfully prepared porous polydivinylbenzene (PDVB) based solid strong acid (PDVB-SO<sub>3</sub>H - SO<sub>2</sub>CF<sub>3</sub>) by grafting of strong electron withdrawing group of SO<sub>2</sub>CF<sub>3</sub> onto the network of performed porous solid acid of PDVB-SO<sub>3</sub>H, which could be synthesized from sulfonation of superhydrophobic porous PDVB or copolymerization of DVB with sodium p-styrene sulfonate. Caio Tagusagawa et al.<sup>17</sup> prepared several porous Ta-W mixed oxides solid acid from TaCl<sub>5</sub> and WCl<sub>6</sub> in the presence of poly block copolymer surfactant pluronic P-123. Although the catalytic application effect was obvious, the catalysts were prepared in harsh reaction conditions and it was hard to control the morphology of the product. To overcome the problems, our groups<sup>18,19</sup> had worked in two aspects. On the one hand, two acid-chromic chloride bi-functionalized catalysts i.e ATP-SO<sub>3</sub>H-Cr(III) and HNTs-SO<sub>3</sub>H-Cr(III) were successfully synthesized by grafting the -SO<sub>3</sub>H and Cr(III) onto the surface of treated attapulgite (ATP) and halloysite nanotubes (HNTs), respectively. On the other hand, based on HNTs by precipitation polymerization and Pickering emulsion polymerization, two polymeric solid acid catalysts i.e. HNTs-polystyrene (PSt)-polydivinylbenzene (PDVB)-SO<sub>3</sub>H(I) and HNTs-PSt-PDVB-SO<sub>3</sub>H(II) were successfully prepared after sulfonation by 98% H<sub>2</sub>SO<sub>4</sub>, respectively. Then, the emulsion templates method<sup>20</sup> is easier and more convenient way to synthesize the porous solid acid material, which was found.

The high internal phase emulsions (HIPEs) with the controlled volume fraction of droplet higher than 74% were adopted to synthesize porous solid acid catalyst materials and subsequent polymerization of the continuous phase commonly known as polyHIPEs.<sup>21</sup> What's more, the porous structure is adjustable by changing the volume ratio of the oil and water phase. However, the traditional polyHIPEs synthesized from surfactants such as span 80 with the amount of between 5 and 50%<sup>22</sup> stabilized water-in-oil (W/O) HIPEs have poor mechanical properties.<sup>23</sup> But poor mechanical properties for polyHIPEs can be improved by increasing the continuous organic phase volume, using particle reinforcements or by changing the composition of the monomer.<sup>24</sup> Among them, increasing small amounts of non-ionic polymeric surfactant to W/O particle-stabilized HIPE templates (Pickering-HIPEs) can lead to the formation of poly-Pickering-HIPEs with an open porous structure and highly mechanical properties.<sup>25</sup> To the best of our knowledge, the use of Pickering HIPEs to produce the porous polymer solid acid catalyst is rarely reported.

Inspired from the discussion above, PDVB-SS-X-SO<sub>3</sub>H (X stand for the volume of span 80 and X = 0, 0.2, 0.6) with open-cell structure, interconnecting pores and strong acidity were designed and synthesized by applying to Pickering HIPEs template method. Firstly, the Stöber's method modified hydrophobic silica particle<sup>26</sup> and span 80 were both used to stabilize W/O Pickering HIPEs with 84.8% the internal phase, and the internal (water) phase contained K<sub>2</sub>SO<sub>4</sub> and sodium p-styrene sulfonate (SS) and the external (oil) phase consisted of divinylbenzene (DVB) and  $\alpha,\alpha'$ -azoisobutyronitrile (AIBN) were emulsified to form stable W/O Pickering HIPEs. Then poly-Pickering-HIPEs were sulfonated by 98% H<sub>2</sub>SO<sub>4</sub> to introduce the group of -SO<sub>3</sub>H and PDVB-SS-X-SO<sub>3</sub>H were obtained. The morphology and various properties of PDVB-SS-X-SO<sub>3</sub>H

were characterized and the catalytic activity PDVB-SS-X-SO<sub>3</sub>H were discussed in detail by optimizing the reaction time, temperature and catalysts loading amounts in catalyzing cellulose to HMF (Scheme 1). What's more, PDVB-SS-X-SO<sub>3</sub>H showed good recyclability and chemical stability.

## 2 Experimental

### 2.1 Chemical and reagents

All the reagents were of analytical grade and used without further purification through purchasing. tetraethoxysilane (TEOS), DVB, formic acid, levulinic acid, 5-HMF (>99%), 1-ethyl-3-methyl-imidazolium chloride ([Emim]Cl, >99%), azobisisobutyronitrile (AIBN), 3-methacryloxypropyltrimethoxysilane (KH-570), cellulose, toluene, ethanol, methanol, Span 80, K<sub>2</sub>SO<sub>4</sub>, potassium persulfate (KPS), NH<sub>3</sub>·H<sub>2</sub>O (25 wt%), sodium p-styrene sulfonate (SS), and acetone were purchased from Aladdin reagent CO., LTD (Shanghai, China).

### 2.2 Instruments

Infrared spectra (4000-400 cm<sup>-1</sup>) was recorded on a Nicolet NEXUS-470 FTIR apparatus (U.S.A.). The morphology of PDVB-SS-X-SO<sub>3</sub>H was observed by field emission scanning electron microscopy (SEM, JSM-7100F). The image of the silica particles was obtained by transmission electron microscope (TEM, JEM-2100). The optical micrographs of Pickering HIPEs were collected by a DMM-330C optical microscope equipped with a high performance digital camera (CAIKON, China). X-ray photoelectron spectroscopy (XPS) of PDVB-SS-X-SO<sub>3</sub>H was recorded by the vario EL III elemental analyzer (Elementar, Hanau, Germany). The acid of PDVB-SS-X-SO<sub>3</sub>H were measured by the instrument of NH<sub>3</sub> temperature-programmed desorption (NH<sub>3</sub>-TPD, finesorb3010). The water contact angle of silica nanoparticles were measured through the Optical Contact Angle Measuring Device (KSV CM200). Detailed test procedure was described as follow. Firstly, silica nanoparticles sample plates were prepared by spreading a thin layer of silica nanoparticles with double-sided adhesive tape on the glass, succedently 2.0 μL of deionized water was injected on the sample surface through the syringe pump, then the images of the water droplet were obtained using the camera in measuring device after the water droplet was formed on the sample surface about 30s. Finally, these images were analyzed using the supplied software to determine the contact angle of sample.

### 2.3 Synthesis and hydrophobic modification of silica nanoparticles

Synthesis of silica nanoparticles by hydrolysis and condensation reaction was implemented according to the previous literature with a slight modification.<sup>26</sup> As a typical run, 6.0 mL of TEOS was added into solution containing of 90 mL of alcohol and 10 mL of H<sub>2</sub>O, and then 3.14 mL of NH<sub>3</sub>·H<sub>2</sub>O with 25 wt% was slowly injected into the mixture at 30 °C, and the reaction were proceeded for 1.0 h under the mechanical stirring. Next, the reaction products were washed with alcohol for several times by centrifugation, and subsequently drying at 80 °C for 3.0 h in drying oven. Finally, the uniform size of silica nanoparticles were obtained.

Silica nanoparticles were further modified to reach hydrophobic. A typical procedure was detailed as follows: Firstly, the mixture silica nanoparticles (1.0 g), toluene (150 mL), H<sub>2</sub>O (15 mL), and KH-570 (3.5 mL) were stirred for 24 h at 40 °C, then the reaction products were washed with alcohol for several times by centrifugation, and dried at 80 °C for 3.0 h in drying oven. Finally, hydrophobic silica nanoparticles were obtained.

#### 2.4 Synthesis of PDVB-SS-X-SO<sub>3</sub>H

For fabrication a stable W/O Pickering HIPEs, the recipes of the aqueous phase and the organic phase were listed in Table 1, and two phases were mixed to achieve homogeneous W/O Pickering HIPEs, respectively. Firstly, the aqueous phase was drop by drop added to the organic phase with a fast and continuous stirring. Secondly, the HIPEs were transferred into plastic centrifuge tube and polymerized in a circulating air oven at 60 °C for 12 h. Then the obtained poly-Pickering-HIPEs were dried at 30 °C for 24 h in a vacuum oven, until a constant weight was achieved. The small molecules in poly-Pickering-HIPEs were removed by Soxhlet extraction in deionized water at 80 °C for 24 h, and then in acetone for an additional at 80 °C for 24 h. Finally, the poly-Pickering-HIPEs which named as PDVB-SS-X (X standing for the volume of Span 80 and X = 0, 0.2, 0.6) were drying at 80 °C for 12 h.

For preparation of sulfonated solid acid catalysts, PDVB-SS-X were sulfonated by the aromatic substitutions in 98% H<sub>2</sub>SO<sub>4</sub>. As a typical run, the mixtures of 1.0 g of PDVB-SS-X particle, and 30 mL of 98% H<sub>2</sub>SO<sub>4</sub> were continuous stirred at 70 °C for 12 h. The reaction products were filtered, repeatedly washed deionized water to remove the excess of H<sub>2</sub>SO<sub>4</sub>, and then dried in vacuum at 80 °C for 3.0 h. Finally, the PDVB-SS-X-SO<sub>3</sub>H were obtained.

#### 2.5 The conversation of cellulose to HMF

The progress of cellulose to HMF was implemented according to the previous literature with a slight modification.<sup>27</sup> As a typical run, the pretreatment of degraded cellulose was performed by adding 0.1 g of D-cellulose powder and 2.0 g of [Emim]Cl into 15 mL of round-bottom flask, and stirring the mixture at 120 °C for 30 min, which resulted in the hydrogen bonds of the cellulose molecules were destroyed, and the degree of crystallization and regularity of the cellulose molecules were reduced. Then, the 40 mg of sulfonated PDVB-SS-X-SO<sub>3</sub>H was added into the mixed solution, and the cellulosic reaction was further carried out at 120 °C for 2.0 h. Finally, the reaction products were diluted for 5000 times in deionized water, and the concentration of HMF was analyzed by 1200 Agilent High Performance Liquid Chromatography (HPLC) equipped with Agilent TC-C18 Column (4.6 × 250 mm, 5.0 mm) and UV detector. During analysis procedure, 20 μL of HMF samples were injected manually and separated through the Agilent TC-C18 column and detected by a UV-vis spectrophotometer at 283 nm. The column temperature was set at 25 °C, and the flow rate of optimized mobile phase consisted of water and methanol with the volume ratio at 30 : 70 was set at 0.7 mL min<sup>-1</sup>. Then, based on the standard curve obtained with the standard substances, the concentration of HMF were obtained, and the HMF yield (Y, mol%) were calculated accord to the following equation:

$$Y\% = \frac{n_1}{n_0} \times 100\%$$

$n_1$  (mol) and  $n_0$  (mol) are the moles of HMF and the moles of glucose units of initial cellulose.

### 3 Results and discussion

#### 3.1 Fabrication of hydrophobic silica nanoparticles

The morphologies of silica nanoparticles and modified silica nanoparticles were both observed by TEM. As shown in Fig. 1a and 1b, silica nanoparticles and hydrophobic silica nanoparticles samples all exhibited a sphere-shaped morphology with similar particle sizes (around 100 ± 20

nm). It was clearly seen that the surface of silica nanoparticles was smooth. But the surface of hydrophobic silica nanoparticles had pale shadow on their rough surface, and some of those were linked together, suggesting the vinyl groups may be grafted on surface of silica nanoparticles. The image of the water contact angle of silica nanoparticles and hydrophobic silica nanoparticles were showed in Fig. 1c and 1d. The values of silica nanoparticles with  $34.7^\circ$  and hydrophobic silica nanoparticles with  $123.2^\circ$  further illustrated the success of modification with vinyl groups. What's more, the hydrophobic silica nanoparticles were proper to stabilize W/O HIPEs, which was proved by Binks's work about using the particles with the water contact angle of  $123^\circ$  to stabilize W/O HIPEs.<sup>28</sup>

### 3.2 Formation of Pickering W/O HIPEs.

In this work, process of preparing Pickering W/O HIPEs and PDVB-SS-0.2-SO<sub>3</sub>H were showed in Fig. 2. The internal (water) phase contained 80 mg of K<sub>2</sub>SO<sub>4</sub>, 40 mg of KPS and 200 mg of SS in 16.8 mL H<sub>2</sub>O, and the external (oil) phase consisted of 3.0 mL of DVB, 40 mg of AIBN, 200 mg of hydrophobic silica nanoparticles, and 0.2 mL of span 80, when the internal and external were mixed, the phase-separated system were formed (Fig. 2a). Then, a stable Pickering W/O HIPE with the internal phase volume fraction of 84.8% was prepared after emulsification (Fig. 2b). Digital photographs of the drops of Pickering HIPEs dispersing in water and toluene were showed in Fig. 2c to test the type of the emulsions, respectively. The drops of the emulsions were diffused in toluene and maintained the original shape, indicating the formation of W/O Pickering HIPEs. In addition, the micrograph of the Pickering W/O HIPEs showed in Fig. 2d, and the uniform and compact liquids revealed the typical type of HIPEs. The morphology of HIPEs was also observed by Xiaodong Li et al.<sup>29</sup> Digital photographs of PDVB-SS-0.2-SO<sub>3</sub>H monolith soaking in water were showed in Fig. 2e. As showed in Fig. 2e, huge water permeated into PDVB-SS-0.2-SO<sub>3</sub>H monolith by pressing into the water via external force, which indicated that a large number of interconnected pores existed inside of PDVB-SS-0.2-SO<sub>3</sub>H monolith.

### 3.3 Characterizations of PDVB-SS-X-SO<sub>3</sub>H

Fig. 3 showed the SEM images of PDVB-SS-0 (a), PDVB-SS-0-HF (b) (i.e. Poly-Pickering-HIPEs removed silica nanoparticles by HF), the triangular domain of PDVB-SS-0-HF (c), PDVB-SS-0-HF-SO<sub>3</sub>H (d), PDVB-SS-0.2-SO<sub>3</sub>H (e), and PDVB-SS-0.6-SO<sub>3</sub>H (f). Clearly, SEM image (Fig. 3a) displayed PDVB-SS-0 has a closed-cell pore structure (pore size of  $100 \pm 8 \mu\text{m}$ ), but no pore throats were observed, indicating the impermeable nature of PDVB-SS-0. We preliminary gained that the PDVB-SS-0 would have worse of the catalytic activity because the reactants and active sites of PDVB-SS-0-SO<sub>3</sub>H may be isolated by closed-cell pores. A obvious double shell structure composed of poly-SS (PSS) internal layer and PDVB external layer were observed in Fig. 2b, and the formative reason may be that the SS monomers in water phase through phase inversion of process were moved to the interface of oil-water and formed a PSS layer when the polymerization of PDVB-SS-0 emulsion. In addition, enlarging image of the triangular domain of PDVB-SS-0-HF (Fig. 2c), many clear 100 nm pores which formed by corroding the stabilized silica nanoparticles in HF were showed on the surface. And the fact that the stabilized silica particles distributed in triangle region to strengthen the stability of HIPEs was proved. Moreover, Michael S. Silverstein et al.<sup>30</sup> also found same result by TEM. The double shell and small pores structures of PDVB-SS-0-HF increased the odds

of contact with reactants in catalytic reaction. Meanwhile, we further sulfonated the PDVB-SS-0-HF, and discovered by SEM that the morphology structure of PDVB-SS-0-HF-SO<sub>3</sub>H (Fig. 3d) was similar to those of PDVB-SS-0-HF (Fig. 3b), which revealing the sulfonated process had no obvious effect on material morphology. Moreover, the fact also suggested that PDVB-SS-X-SO<sub>3</sub>H had excellent chemical and mechanical stability. With the increase of the volume of span 80, the different pore sizes of PDVB-SS-0-HF-SO<sub>3</sub>H (Fig. 3d), PDVB-SS-0.2-SO<sub>3</sub>H (Fig. 3e) and PDVB-SS-0.6-SO<sub>3</sub>H (Fig. 3f) were obtained and were about 100 μm, 10 μm and 50 μm, respectively. The difference results of our observation may be attributable to three reasons, firstly, the adsorption of surfactant on particles promoted their attachment to the drop interface, leading to decrease the droplets size. Secondly, increasing the surfactant concentration lowered the oil-water interfacial tension, which facilitating drop break up during emulsification.<sup>31</sup> Thirdly, instability the droplets of the W/O Pickering HIPEs combined each other during polymerization process leading to form bigger pore sizes. These similar results have been also reported by Wong et al.<sup>32</sup>

Energy Dispersive Spectrometer (EDS) analysis equipped with SEM for PDVB-SS-0, PDVB-SS-0-HF, PDVB-SS-0-SO<sub>3</sub>H, PDVB-SS-0-HF-SO<sub>3</sub>H, PDVB-SS-0.2-SO<sub>3</sub>H, and PDVB-SS-0.6-SO<sub>3</sub>H were listed in Fig. 4a-4f, respectively. When compared with Fig. 4a and Fig. 4b, the peak of element Si of PDVB-SS-0-HF was disappeared, and same phenomenon of PDVB-SS-0-HF-SO<sub>3</sub>H was also appeared when compared with Fig. 4c and Fig. 4d, which suggested the silica nanoparticles were successfully removed. Interestingly, as shown the peaks of elements S from Fig. 4a-4d, the peaks of element S of PDVB-SS-0-SO<sub>3</sub>H and PDVB-SS-0-HF-SO<sub>3</sub>H were stronger than those of PDVB-SS-0 and PDVB-SS-0-HF, respectively, which indicating that the internal phase SS monomers were successfully polymerized into PSS, and -SO<sub>3</sub>H group were also grafted on PDVB via sulfonation process. Additionally, this fact could be further proved the result of SEM about the formation of PSS layer. The peaks of elements S, O from PDVB-SS-0.6-SO<sub>3</sub>H (Fig. 4f) were both evident stronger than those of PDVB-SS-0.2-SO<sub>3</sub>H (Fig. 4e). This result can be attributed to the formation of larger cell structure by Pickering HIPEs templates in the presence of more content span 80, and the large pore was easier to be grafted by -SO<sub>3</sub>H groups. Moreover, the results of element analysis for PDVB-SS-0, PDVB-SS-0-HF, PDVB-SS-0-SO<sub>3</sub>H, PDVB-SS-0-HF-SO<sub>3</sub>H, PDVB-SS-0.2-SO<sub>3</sub>H, and PDVB-SS-0.6-SO<sub>3</sub>H were also shown in the corresponding figures, respectively. Moreover, the weight of S of PDVB-SS-0-SO<sub>3</sub>H (0.65%), PDVB-SS-0-HF-SO<sub>3</sub>H (0.98%) and PDVB-SS-0.6-SO<sub>3</sub>H (2.62%) were increased to those of PDVB-SS-0 (0.06%), PDVB-SS-0-HF (0.09%) and PDVB-SS-0.2-SO<sub>3</sub>H (1.09%), respectively, since -SO<sub>3</sub>H groups were successfully grafted onto PDVB-SS-X-SO<sub>3</sub>H. This fact was matched to the results EDS analysis.

Fig. 5 showed the FT-IR spectra of PDVB-SS-0-HF-SO<sub>3</sub>H (a) and PDVB-SS-0-SO<sub>3</sub>H (b), respectively. The peaks of 1039 cm<sup>-1</sup>, 1170 cm<sup>-1</sup> and 1487 cm<sup>-1</sup> which associated with C-S bond, -SO<sub>3</sub>H group and benzene ring could be clearly found in the samples of PDVB-SS-0-HF-SO<sub>3</sub>H and PDVB-SS-0-SO<sub>3</sub>H, suggesting the presence of sulfonic group and benzene ring in these samples.<sup>33</sup> The band around 1107 cm<sup>-1</sup> associated with Si-O-Si antisymmetric stretching vibration was only found in the sample of PDVB-SS-0-SO<sub>3</sub>H, suggesting the silica nanoparticles were completely washed out by HF for the samples of PDVB-SS-0-HF-SO<sub>3</sub>H. This result was matched to the results of element analysis and EDS analysis.

Fig. 6 showed the X-ray photoelectron spectroscopy (XPS) measurements of

PDVB-SS-0-HF-SO<sub>3</sub>H and PDVB-SS-0-SO<sub>3</sub>H, respectively. Clearly, PDVB-SS-0-HF-SO<sub>3</sub>H and PDVB-SS-0-SO<sub>3</sub>H both showed the signals of S, C and O, possibly indicating the presence of -SO<sub>3</sub>H group in these samples. Correspondingly, the high resolved XPS spectrum of C1s showed the signals at around 284.7 and 275.4 eV associated with C-C and C-S bond could be found in these samples, further suggesting the successful introduction of -SO<sub>3</sub>H onto the network of PDVB-SS-X-SO<sub>3</sub>H, and -SO<sub>3</sub>H group played a key factor for increasing the acid strength of PDVB-SS-X-SO<sub>3</sub>H. The signal of S2p of PDVB-SS-0-HF-SO<sub>3</sub>H and PDVB-SS-0-SO<sub>3</sub>H were found in same position with binding energy 169 eV, suggesting no obvious effect of sulfonating process for PDVB-SS-X-SO<sub>3</sub>H after removing silica nanoparticles by HF. The results also supported the fact that PDVB-SS-X-SO<sub>3</sub>H possessed rigid network structure and good chemical stability, which also were proved based on the above morphology structure analysis of PDVB-SS-0-HF and PDVB-SS-0-HF-SO<sub>3</sub>H.

The acidic features of PDVB-SS-0-SO<sub>3</sub>H, PDVB-SS-0-HF-SO<sub>3</sub>H, PDVB-SS-0.2-SO<sub>3</sub>H, and PDVB-SS-0.6-SO<sub>3</sub>H solid catalysts were determined by means of NH<sub>3</sub>-TPD, respectively. For the desorbed NH<sub>3</sub>, the physically adsorbed and hydrogen-bonded NH<sub>3</sub> can desorb at ≤150 °C,<sup>34</sup> and the acid site bound resulted in other desorbed NH<sub>3</sub> at the higher temperatures.<sup>35</sup> In addition, the desorbed NH<sub>3</sub> at desorption temperatures of 150-250 °C, 250-350 °C, 350-500 °C and >500 °C were measured as weak, medium, strong and very strong of the acid sites, respectively.<sup>36</sup> As shown in Fig. 7, it can be clearly seen that medium, strong and very strong acid sites existed in PDVB-SS-X-SO<sub>3</sub>H, and the areas of the peaks represented the amount of acidic sites which were calculated and summarized in Table 2, respectively. The total acidic amount of PDVB-SS-0-SO<sub>3</sub>H, PDVB-SS-0-HF-SO<sub>3</sub>H, PDVB-SS-0.2-SO<sub>3</sub>H, and PDVB-SS-0.6-SO<sub>3</sub>H were 170 μmol g<sup>-1</sup> (i.e. respective acidic amounts of 25 μmol g<sup>-1</sup>, 69 μmol g<sup>-1</sup>, and 76 μmol g<sup>-1</sup> for the acidic strengths of 300 °C, 470 °C and 578 °C), 207 μmol g<sup>-1</sup> (i.e. respective acidic amounts of 48 μmol g<sup>-1</sup>, 76 μmol g<sup>-1</sup>, and 83 μmol g<sup>-1</sup> for the acidic strengths of 289 °C, 420 °C and 578 °C), 233 μmol g<sup>-1</sup> (i.e. respective acidic amounts of 46 μmol g<sup>-1</sup>, 92 μmol g<sup>-1</sup>, and 95 μmol g<sup>-1</sup> for the acidic strengths of 275 °C, 379 °C and 548 °C), and 244 μmol g<sup>-1</sup> (i.e. respective acidic amounts of 34 μmol g<sup>-1</sup>, 69 μmol g<sup>-1</sup>, and 141 μmol g<sup>-1</sup> for the acidic strengths of 284 °C, 359 °C and 508 °C), which was suitable to the results of the content of S with 0.65%, 0.98%, 1.09%, and 2.62% by elemental analysis, respectively. The acidic amount provides a number of acidic sites, and the acidic sites can help to improve efficiency to cellulose to HMF.<sup>37</sup> In a word, PDVB-SS-X-SO<sub>3</sub>H had much strong acidic sites and the existence of the strong acidic feature i.e. 145 μmol g<sup>-1</sup> at 470 °C and 578 °C for PDVB-SS-0-SO<sub>3</sub>H, 159 μmol g<sup>-1</sup> at 420 °C and 578 °C for PDVB-SS-0-HF-SO<sub>3</sub>H, 187 μmol g<sup>-1</sup> at 379 °C and 548 °C for PDVB-SS-0.2-SO<sub>3</sub>H, and 210 μmol g<sup>-1</sup> at 359 °C and 508 °C for PDVB-SS-0.6-SO<sub>3</sub>H, which could be effective to catalyze the reaction of cellulose to HMF.

#### 3.4 Conversion of cellulose to HMF using PDVB-SS-X-SO<sub>3</sub>H as the catalyst

The optimal reaction conditions about cellulose to HMF using PDVB-SS-0.2-SO<sub>3</sub>H as the catalyst were found by the experience, and the specific optimization reaction progress was listed as follows: firstly, cellulose (100 mg) was pretreatment in [Emim]Cl (2.0 g) at 120 °C for 0.5 h. Then the catalyst (40 mg) was added into the reactor and kept for another 3.0 h in same condition. The effect of the different quality of catalyst for the yield of HMF from cellulose on same condition was studied, and the results were showed in Fig. 8a. It could be observed that only 9.8%

yield of HMF was obtained when 20 mg of PDVB-SS-0.2-SO<sub>3</sub>H was used at 120 °C for 2.0 h, but the yield of HMF unexpectedly reached to 29.6% as the amount of PDVB-SS-0.2-SO<sub>3</sub>H increased to 40 mg, and the amount of catalyst was much lower than those of Wang Pan.<sup>38</sup> This fact indicated that addition of PDVB-SS-0.2-SO<sub>3</sub>H showed excellent catalytic performance about degrading cellulose to HMF. It may be because the increasing catalytic sites boost the dehydration reaction with the increasing amount of catalyst. However, when the amount of catalyst increased from 40 mg to 60 mg, there was a smooth decrease in HMF yield. The same tendency of the HMF yield with the increasing catalytic was also found by Hu's group.<sup>39</sup> This phenomenon implied that the side reaction of cellulose-degradation also accelerated under over-using of catalysts, which probably facilitated the decomposition of HMF or the polymerization of HMF.<sup>40</sup> Moreover, the addition of excess catalysts limited the mass transfer and decreased the amount of cellulose to join in reaction at the same time.<sup>41</sup>

Meanwhile, we also studied the effects of reaction temperature and time on the yield of HMF from cellulose, and the results were showed in Fig. 8b. Under same reaction time (i.e. 2.0 h and 40 mg of catalyst), the 29.6% HMF yield at 120 °C was much higher than the 15.3% HMF yield at 110 °C, the 21.6% HMF yield at 130 °C, and the 25.7% HMF yield at 140 °C, which indicated that reaction temperature has a great influence on the HMF yield. Proper high reaction temperature can accelerate the degrading of cellulose, and the descending trend was more obvious with higher reaction temperature, which suggested that higher reaction temperature can improve the rehydration and polycondensation of HMF to undesired byproducts, such as soluble polymers and insoluble humins. What's more, the same results were also found by Zhou's group.<sup>42</sup> There were two possible reasons. Firstly, the increasing reaction temperature reduced the viscosity of ionic liquids and increased contact area between catalyst and the reactants, which was benefit for accelerate the degradation of cellulose. Secondly, the by-product of HMF covered the acid sites of catalysts, and the reaction of HMF to other substances was enhanced with the further increasing reaction temperature. And furthermore, the by-products including formic acid and levulinic acid were examined by HPLC, and Zakrzewska's work also reported that HMF was decomposed to some unidentified products.<sup>43</sup>

To discuss the possible influence factor to the conversion of cellulose to HMF, the HMF yield of PDVB-SS-0-SO<sub>3</sub>H (12.9%), PDVB-SS-0-HF-SO<sub>3</sub>H (20.6%), PDVB-SS-0.2-SO<sub>3</sub>H (29.6%) and PDVB-SS-0.6-SO<sub>3</sub>H (15.5%) in same condition (40 mg of catalyst, 2.0 h of reaction time, and 120 °C of reaction temperature) were obtained and also listed in Table 2, respectively. It is clear that PDVB-SS-0.2-SO<sub>3</sub>H obtained higher HMF yield. Moreover, according to the performance of PDVB-SS-X-SO<sub>3</sub>H of the above discussion, we also knew that PDVB-SS-0.2-SO<sub>3</sub>H had smaller pore sizes (about 10 μm) and moderate amount of strong acid (187 μmol g<sup>-1</sup>). So we concluded that the results may be attributed to two aspects: firstly, the smaller pore sizes helped to increase contact frequency between reaction substrates and catalytic acid sites. Secondly, moderate amount of strong acid more conducive to improve the catalytic effect of cellulose to HMF.

### 3.5 Recycling of catalysis system

The recyclability of catalyst was very important to the practical production of HMF, and was fit the demand of green and sustainable chemistry. Therefore, the recycling activity of the catalyst was examined with a set of experiments. The solid acid catalyst PDVB-SS-0.2-SO<sub>3</sub>H were

recovered by filtering the mixture after the first reaction end, washing 10 times with 5.0 mL deionized water, and drying at 30 °C for 24 h in a vacuum oven. Subsequently, the solid acid catalysts were used to the reaction of cellulose to HMF for four times at same condition, and the yields of HMF were 23.4%, 22.6%, 21.4%, and 20.3%, respectively. The loss of -SO<sub>3</sub>H and the deposition of humins on the surface the solid acid catalysts can lead to the decrease of HMF yield, but the catalyst still have a good activity after repeating four time. Thus the system of PDVB-SS-X-SO<sub>3</sub>H can be effectively reused.

#### 4 Conclusion

In this work, PDVB-SS-X-SO<sub>3</sub>H having adjustable porous structure were successfully synthesized by applying Pickering HIPEs template, and then PDVB-SS-X-SO<sub>3</sub>H were used as solid super-acidic catalysts to produce the HMF from cellulose in ionic liquid system. The porous properties and acidic features of the PDVB-SS-X-SO<sub>3</sub>H were characterized, and the amount of catalyst (40 mg), reaction time (2.0 h), and reaction temperature (120 °C) were optimized to cellulosic conversion in the presence of PDVB-SS-0.2-SO<sub>3</sub>H. The 29.6% yield of HMF was produced in the PDVB-SS-0.2-SO<sub>3</sub>H catalyzed system, which was superior to the PDVB-SS-0.6-SO<sub>3</sub>H system with 15.5%, PDVB-SS-0-HF-SO<sub>3</sub>H system with 20.6%, and PDVB-SS-0-SO<sub>3</sub>H system with 12.9%. It could be concluded that the pore sizes and acidic features of PDVB-SS-X-SO<sub>3</sub>H was important for cellulose to HMF. This work was continued to effort to make macroporous polymerized solid acid, and the results of this work provided for a few useful experiences for future research towards development of new energy, especially in their wide application for bioenergy.

#### Acknowledgements

This work was financially supported by the National Natural Science Foundation of China (no. 21107037, no.21176107, no. 21306013), Natural Science Foundation of Jiangsu Province (no.BK20131223), National Postdoctoral Science Foundation (no. 2013M530240), Special National Postdoctoral Science Foundation (no. 2014T70480), Postdoctoral Science Foundation funded Project of Jiangsu Province (no. 1202002B) and Programs of Senior Talent Foundation of Jiangsu University (no. 12JDG090).

#### References

- 1 D. M. Alonso, J. Q. Bond and J. A. Dumesic, *Green Chem.*, 2010, 12, 1493-1513
- 2 L. Hu, G. Zhao, W. W. Hao, X. Tang, Y. Sun, L. Lin and S. J. Liu, *RSC Adv.*, 2012, 2, 11184-11206.
- 3 L. Y. Roman, C. J. Barrett and Z. Y. Liu, *Nature*, 2007, 447, 982-985.
- 4 M. Balakrishnan, E. R. Sacia and A. T. Bell, *Green Chem.*, 2012, 49, 1626-1634.
- 5 K. M. Rapp, US 4740605, 1988-04-26.
- 6 F. S. Asghari and H. Yoshida, *Ind. Eng. Chem. Res.*, 2006, 45, 2163-2173.
- 7 Jiménez-Morales, J. santamaria-González, P. Maireles-Torres and A. Jiménez-López, *Applied Catalysis B: Environmental*, 2011, 103, 91-98.
- 8 L. A. S. do Nascimento, L. M. Z. Tito, T. S. Angelica, C. E. F. da Costa, J. R. Zamian and G. N. da Rocha Filho, *Applied Catalysis B: Environmental*, 2011, 101, 495-503.
- 9 B. V. S. K. Rao, K. C. Mouli, N. Rambabu, A. K. Dalai and R. B. N. Prasad, *Catalysis Communications*, 2011, 14, 20-26.
- 10 M. Toda, A. Takagaki, M. Okamura, J. N. Kondo, K. Domen, S. Hayashi and M. Hara, *Nature*,

- 2005, 438, 178-178.
- 11 G. Pasquale, P. Vázquez, G. Romanelli, G. Baronetti, *Catalysis Communications*, 2012, 18, 115-120.
  - 12 C. Tagusagawa, A. Takagaki, K. Takanabe, K. Ebitani, S. Hayashi and K. Domen, *Journal of Catalysis*, 2010, 270, 206-212.
  - 13 Z. H. Zhang, K. Dong and Z. K. Zhao, *ChemSusChem*, 2011, 4, 112-118.
  - 14 L. Hu, G. Zhao, X. Tang, Z. Wu, J. X. Xu, L. Lin and S. J. Liu, *Bioresource Technology*, 2013, 148, 501-507.
  - 15 J. Liu, W. P. Kong, C. Qi, L. F. Zhu and F. S. Xiao, *ACS Catal.*, 2012, 2, 565-572.
  - 16 F. Liu, *Applied Catalysis B: Environmental*, 2013, 136, 193-201.
  - 17 C. Tagusagawa, A. Takagaki, A. Iguchi, K. Takanabe, J. N. Kondo, K. Ebitani, T. Tatsumi, and K. Domen, *Chem. Mater.*, 2010, 22, 3072-3078.
  - 18 Y. L. Zhang, J. M. Pan, Y. S. Yan, W. D. Shi and L. B. Yu, *RSC Adv.*, 2014, 4, 23797-23806.
  - 19 Y. L. Zhang, J. M. Pan, Y. S. Yan, W. D. Shi and L. B. Yu, *RSC Adv.*, 2013, 4, 11664-11672.
  - 20 Y. Yu, J. W. Zeng, Y. W. Chao and T. Zhen, *Chem. Commun.*, 2013, 49, 7144-7146.
  - 21 N. R. Cameron, *Polymer*, 2005, 46, 1439-1449.
  - 22 S. D. Kimmins and N. R. Cameron, *Adv. Funct. Mater.*, 2011, 21, 211-225.
  - 23 A. Menner, R. Powell, A. Bismarck, *Macromolecules* 2006, 39, 2034-2035.
  - 24 V. O. Ikem, A. Menner, A. Bismarck, *Angew. Chem. Int. Ed.* 2008, 47, 8277-8279.
  - 25 V. O. Ikem, A. Menner, T. S. Horozov and A. Bismarck, *Adv. Mater.* 2010, 22, 3588-3592
  - 26 W. Stöber, A. Fink and E. Bohn, *J. Colloid Interface Sci.*, 1968, 26, 62-69.
  - 27 H. H. Wei, Y. L. Yin, H. P. Wun, and C. W. W. Kevin, *Catalysis Today*, 2011, 174, 65-69
  - 28 B. P. Binks and S. Lumsdon, *Phys. Chem. Chem. Phys.*, 2000, 2, 2959-2967.
  - 29 X. D. Li, G. Q. Sun, Y. C. Li, J. C. Yu, J. Wu, G. H. Ma and T. Ngai, *Langmuir*, 2014, 30, 2676-2683.
  - 30 I. Gurevitch and M. S. Silverstein, *Macromolecules*, 2011, 44, 3398-3409.
  - 31 S. W. Zou, Y. Yang, H. Liu and C. Y. Wang, *Colloids and Surfaces A: Physicochem. Eng. Aspects*, 2013, 436, 1-9
  - 32 L.L.C. Wong, V.O. Ikem, A. Menner and A. Bismarck, *Macromol. Rapid Commun*, 2011, 32, 1563-1568.
  - 33 Scaranto, A. P. Charmet and S. Giorgianni, *Journal of Physical Chemistry C*, 2008, 112, 9443-9447.
  - 34 D. Liu, P. Yuan, H. M. Liu, J. G. Cai, Z. H. Qin, D. Y. Tan, Q. Zhou, H. P. He and J. X. Zhu, *Appl. Clay Sci.*, 2011, 52, 358-363.
  - 35 R. C. Ravindra, Y. S. Bhat, G. Nagendrappa and B. S. Jai Prakash, *Catal. Today*, 2009, 141, 157-160.
  - 36 D. Liu, P. Yuan, H. M. Liu, J. G. Cai, D. Y. Tan, H. P. He, J. X. Zhu and T. H. Chen, *Appl. Clay Sci.*, 2013, 80, 407-412.
  - 37 P. Kalita, B. Sathyaseelan, A. Mano, S. M. Javaid Zaidi, M. A. Chari and A. Vinu, *Chem.Eur.J.*, 2010, 16, 2843-2846.
  - 38 P. Wang, H. B. Yu and S. H. Zhan, *Bioresource Technology*, 2011, 102, 4179-4183.
  - 39 L. Hu, G. Zhao, X. Tang, Z. Wu, J.X. Xu, L. Lin and S.J. Liu, *Bioresource Technology*, 2013, 148, 501-507.
  - 40 Q. Zhao, L. Wang, S. Zhao, X. H. Wang and S. T. Wang, *Fuel*, 2011, 90, 2289-2293.
  - 41 C. Aellig and I. Hermans, *ChemSusChem*, 2012, 5, 1737-1742.
  - 42 L. L. Zhou, R. J. Liang, Z. W. Ma, T. H. Wu and Y. Wu, *Bioresource Technology*, 2013, 129, 450-455.
  - 43 M. E. Zakrzewska, E. Bogel-Lukasik and R. Bogel-Lukasik, *Chem. Rev.*, 2011, 111, 397-417.

Table 1 Recipes of HIPEs

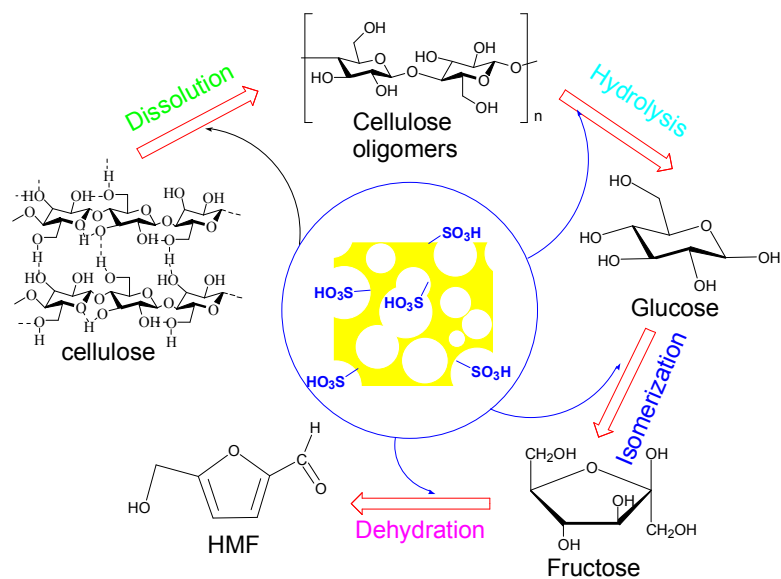
Sample <sup>a</sup>	External, organic phase				Internal, aqueous phase			
	DVB (mL)	AIBN (g)	Silica (g)	Span 80 (mL)	Water (g)	K <sub>2</sub> SO <sub>4</sub> (g)	KPS (g)	SS (g)
PDVB-SS-0-SO <sub>3</sub> H	3.0	0.04	1.0	0	16.8	0.08	0.04	0.2
PDVB-SS-0.2-SO <sub>3</sub> H	3.0	0.04	0.3	0.2	16.8	0.08	0.04	0.2
PDVB-SS-0.6-SO <sub>3</sub> H	3.0	0.04	0.3	0.6	16.8	0.08	0.04	0.2

<sup>a</sup> PDVB-SS-X-SO<sub>3</sub>H, X stand for the volume of Span 80

Table 2 The properties of the catalyst and catalytic efficiency

Sample <sup>a</sup>	Acid strength	Acid amounts	Total acid amounts	HMF
	(°C)	( $\mu\text{mol g}^{-1}$ )	( $\mu\text{mol g}^{-1}$ )	(%)
PDVB-SS-0-SO <sub>3</sub> H	300	25	170	12.9
	470	69		
	578	76		
PDVB-SS-0-HF-SO <sub>3</sub> H	289	48	207	20.6
	420	76		
	578	83		
PDVB-SS-0.2-SO <sub>3</sub> H	275	46	233	29.6
	379	92		
	548	95		
PDVB-SS-0.6-SO <sub>3</sub> H	284	34	244	15.5
	359	69		
	508	141		

<sup>a</sup> PDVB-SS-X-SO<sub>3</sub>H, X stand for the volume of Span 80



Scheme1. PDVB-SS-X-SO<sub>3</sub>H catalyzed conversion of cellulose into HMF in [Emim]Cl under atmospheric pressure.

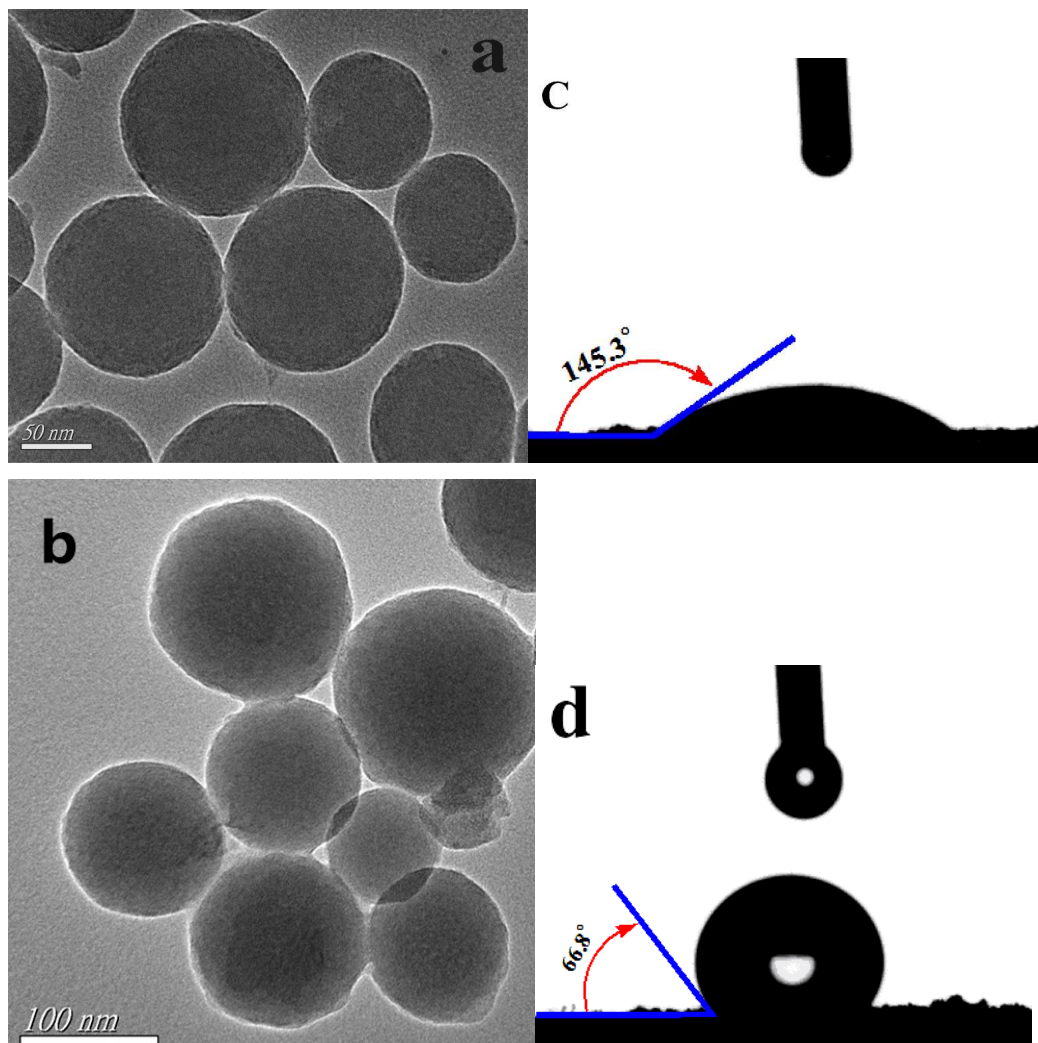


Fig. 1 TEM images of (a) silica nanoparticles, and (c) hydrophobic silica nanoparticles; the contact angles of water images of (b) silica nanoparticles, and (d) hydrophobic silica nanoparticles.



Fig. 2 Exposition of prepared Pickering W/O HIPEs and PDVB-SS-X-SO<sub>3</sub>H using the experimental progress of PDVB-SS-0.2-SO<sub>3</sub>H (a) phase-separated system, (b) Pickering W/O HIPEs with an 84.8 vol % internal phase fraction, (c) the Pickering W/O HIPEs dispersed in water and toluene, respectively, (d) micrograph of the Pickering W/O HIPEs, (e) PDVB-SS-0.2-SO<sub>3</sub>H monolith soaked in water.

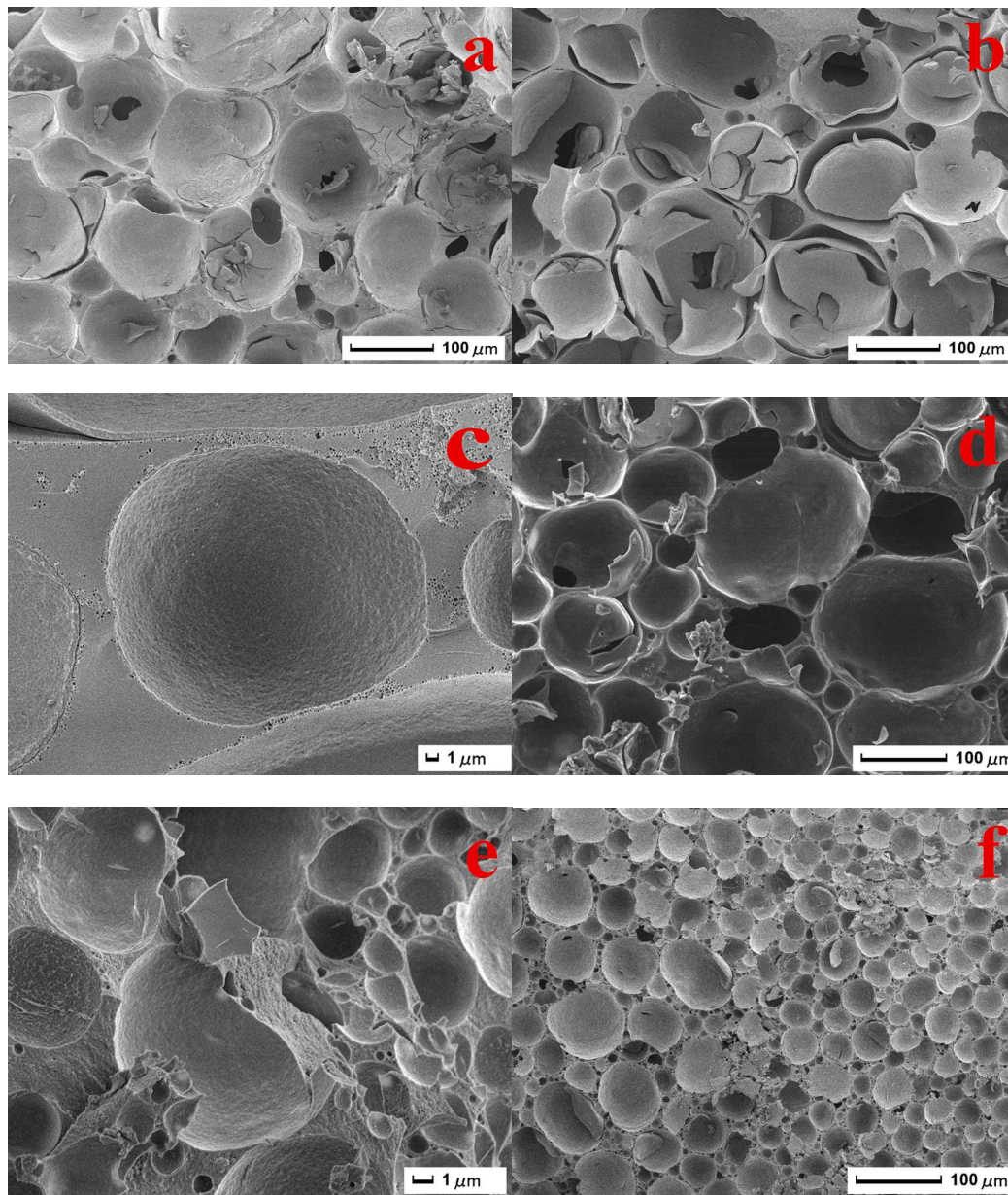


Fig. 3 SEM images of (a) PDVB-SS-0 (b) PDVB-SS-0-HF, (c) the triangular domain of PDVB-SS-0-HF, (d) PDVB-SS-0-HF-SO<sub>3</sub>H, (e) PDVB-SS-0.2-SO<sub>3</sub>H, and (f) PDVB-SS-0.6-SO<sub>3</sub>H.

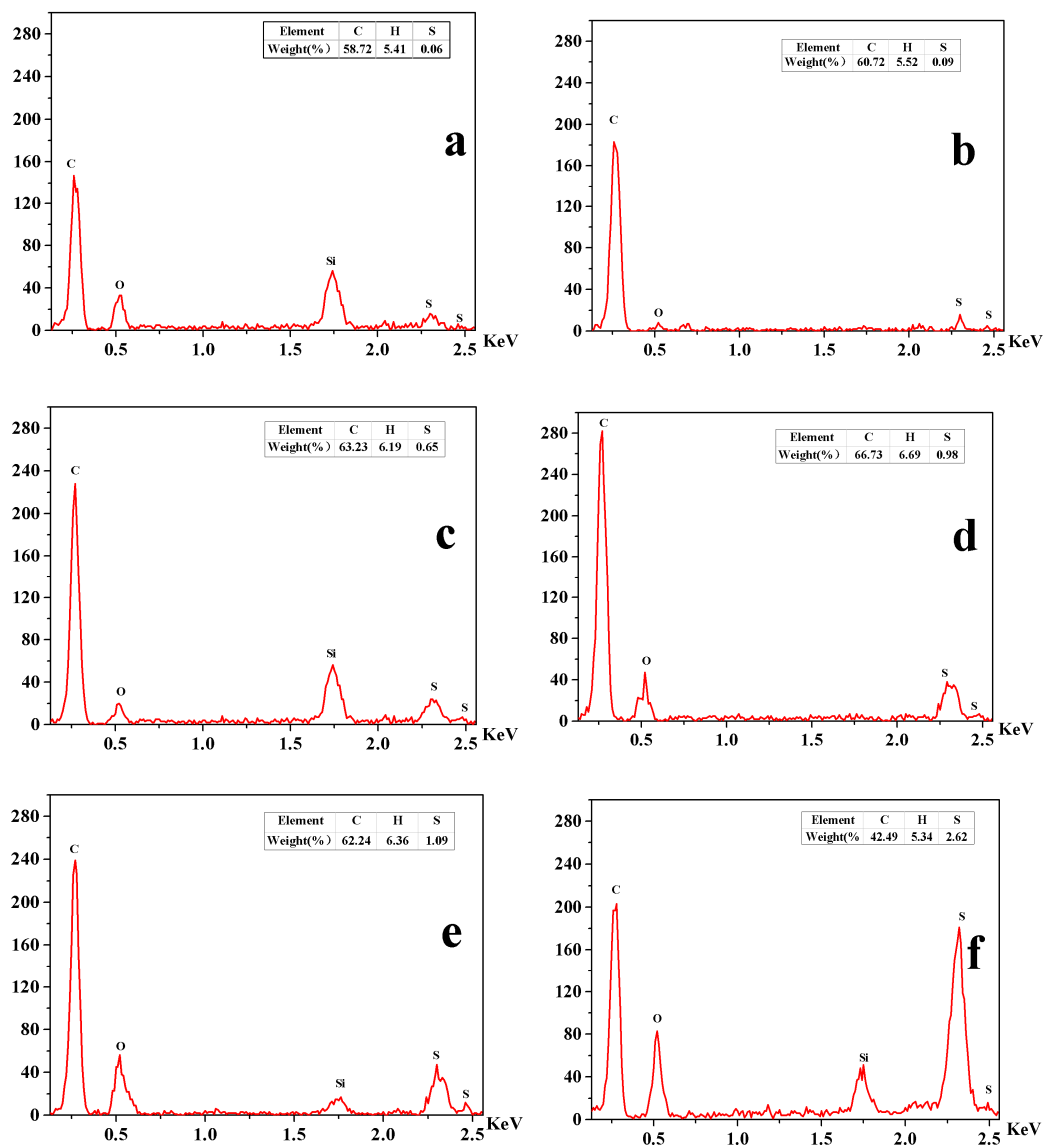


Fig. 4 Energy Dispersive Spectrometer (EDS) and element analysis of (a) PDVB-SS-0 (b) PDVB-SS-0-HF, (c) PDVB-SS-0-SO<sub>3</sub>H, (d) PDVB-SS-0-HF-SO<sub>3</sub>H, (e) PDVB-SS-0.2-SO<sub>3</sub>H, and (f) PDVB-SS-0.6-SO<sub>3</sub>H.

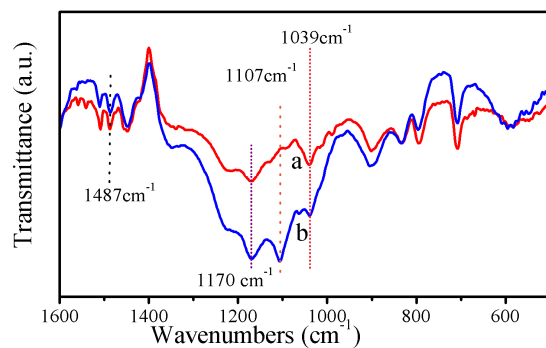


Fig. 5 FT-IR spectra of (a) PDVB-SS-0-HF-SO<sub>3</sub>H, and (b) PDVB-SS-0-SO<sub>3</sub>H.

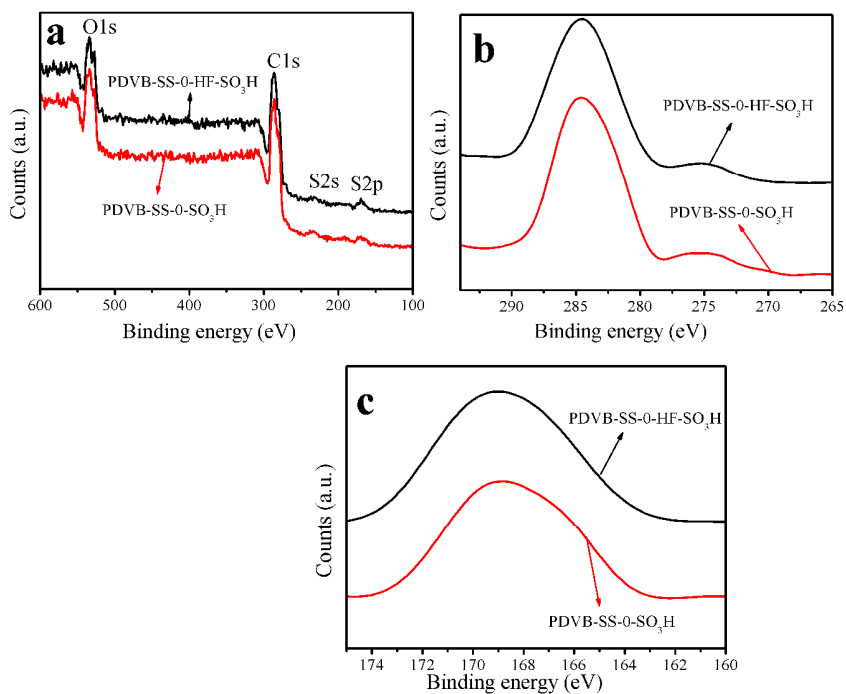


Fig. 6 X-ray photoelectron spectroscopy measurements of (a) survey, (b) C1s, (c) S2p of PDVB-SS-0-HF-SO<sub>3</sub>H and PDVB-SS-0-SO<sub>3</sub>H.

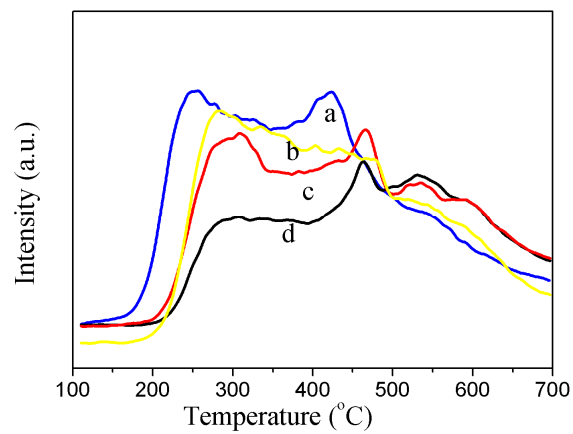


Fig. 7 NH<sub>3</sub>-TPD curves of (a) PDVB-SS-0.2-SO<sub>3</sub>H, (b) PDVB-SS-0.6-SO<sub>3</sub>H, (c) PDVB-SS-0-HF-SO<sub>3</sub>H, and (d) PDVB-SS-0-SO<sub>3</sub>H

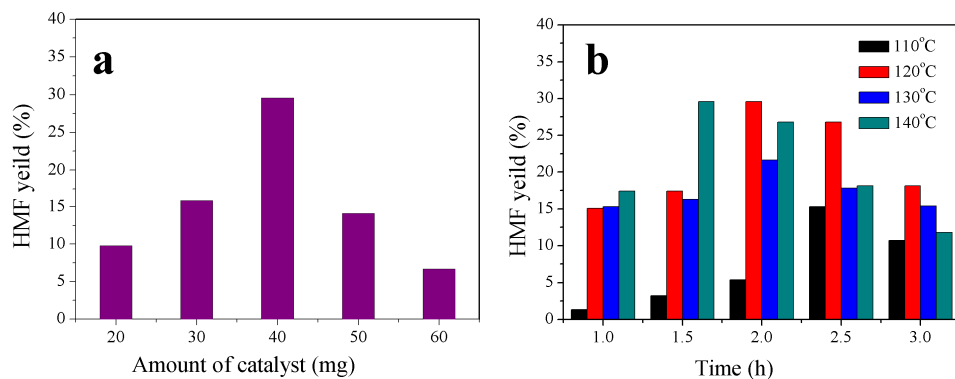


Fig. 8 Optimization of reaction conditions to cellulose to HMF using PDVB-SS-0.2-SO<sub>3</sub>H as the catalyst. The effects of (a) the amount of PDVB-SS-0.2-SO<sub>3</sub>H, and (b) reaction time and temperature under 40 mg of catalyst and 2.0 g of [Emim]Cl.